



University of
Zurich^{UZH}

Zurich Open Repository and
Archive

University of Zurich
University Library
Strickhofstrasse 39
CH-8057 Zurich
www.zora.uzh.ch

Year: 2017

Search for the CP-violating strong decays D^{*+} and $(958)^+$

LHCb Collaboration ; Bernet, R ; Müller, K ; Steinkamp, O ; Straumann, U ; Vollhardt, A ; et al

Abstract: A search for the CP-violating strong decays D^{*+} and $(958)^+$ has been performed using approximately 2.5×10^7 events of each of the decays D^{*++} and D_s^{*++} , recorded by the LHCb experiment. The data set corresponds to an integrated luminosity of 3.0 fb^{-1} of pp collision data recorded during LHC Run 1 and 0.3 fb^{-1} recorded in Run 2. No evidence is seen for $D_{(s)}^{*+} \rightarrow \rho^0 \pi^+$ with $\rho^0 \rightarrow \pi^+ \pi^-$, and upper limits at 90% confidence level are set on the branching fractions, $\mathcal{B}(D^{*+} \rightarrow \rho^0 \pi^+) < 1.6 \times 10^{-5}$ and $\mathcal{B}(D_s^{*+} \rightarrow \rho^0 \pi^+) < 1.8 \times 10^{-5}$. The limit for the $D^{*+} \rightarrow \omega \pi^+$ decay is comparable with the existing one, while that for the $D_s^{*+} \rightarrow \omega \pi^+$ is a factor of three smaller than the previous limit.

DOI: <https://doi.org/10.1016/j.physletb.2016.11.032>

Posted at the Zurich Open Repository and Archive, University of Zurich

ZORA URL: <https://doi.org/10.5167/uzh-129664>

Journal Article

Published Version



The following work is licensed under a Creative Commons: Attribution 4.0 International (CC BY 4.0) License.

Originally published at:

LHCb Collaboration; Bernet, R; Müller, K; Steinkamp, O; Straumann, U; Vollhardt, A; et al (2017). Search for the CP-violating strong decays D^{*+} and $(958)^+$. Physics Letters B, 764:233-240.

DOI: <https://doi.org/10.1016/j.physletb.2016.11.032>



Search for the CP-violating strong decays $\eta \rightarrow \pi^+\pi^-$ and $\eta'(958) \rightarrow \pi^+\pi^-$



The LHCb Collaboration

ARTICLE INFO

Article history:

Received 13 October 2016
Received in revised form 11 November 2016
Accepted 17 November 2016
Available online 23 November 2016
Editor: L. Rolandi

ABSTRACT

A search for the CP-violating strong decays $\eta \rightarrow \pi^+\pi^-$ and $\eta'(958) \rightarrow \pi^+\pi^-$ has been performed using approximately 2.5×10^7 events of each of the decays $D^+ \rightarrow \pi^+\pi^+\pi^-$ and $D_s^+ \rightarrow \pi^+\pi^+\pi^-$, recorded by the LHCb experiment. The data set corresponds to an integrated luminosity of 3.0 fb^{-1} of pp collision data recorded during LHC Run 1 and 0.3 fb^{-1} recorded in Run 2. No evidence is seen for $D_{(s)}^+ \rightarrow \pi^+\eta^{(\prime)}$ with $\eta^{(\prime)} \rightarrow \pi^+\pi^-$, and upper limits at 90% confidence level are set on the branching fractions, $\mathcal{B}(\eta \rightarrow \pi^+\pi^-) < 1.6 \times 10^{-5}$ and $\mathcal{B}(\eta' \rightarrow \pi^+\pi^-) < 1.8 \times 10^{-5}$. The limit for the η decay is comparable with the existing one, while that for the η' is a factor of three smaller than the previous limit.

© 2016 The Author. Published by Elsevier B.V. This is an open access article under the CC BY license (<http://creativecommons.org/licenses/by/4.0/>). Funded by SCOAP³.

1. Introduction

The strength of CP violation in weak interactions in the quark sector is well below what would be required to serve as an explanation for the observed imbalance between the amounts of matter and antimatter in the universe. The QCD Lagrangian could contain a term, the θ term [1], that would give rise to CP violation in strong interactions; however, no strong CP violation has been observed. The experimental upper limit on the neutron electric dipole moment ($nEDM$) implies a limit $\theta \lesssim 10^{-10}$ [2]. The closeness of the value of θ to zero is seen as a fine-tuning problem, the so-called “strong CP problem”. Solutions to the strong CP problem may involve axions [3], extra space–time dimensions [4], massless up quarks [5], string theory [6] or quantum gravity [7].

The decay modes $\eta \rightarrow \pi^+\pi^-$ and $\eta'(958) \rightarrow \pi^+\pi^-$ would both violate CP symmetry. In the Standard Model (SM) these decays could happen via the CP-violating weak interaction, through mediation by a virtual K_S^0 meson, with expected branching fractions $\mathcal{B}(\eta \rightarrow \pi^+\pi^-) < 2 \times 10^{-27}$ and $\mathcal{B}(\eta' \rightarrow \pi^+\pi^-) < 4 \times 10^{-29}$ [8]. Based on the limit from the $nEDM$ measurements, strong decays mediated by the θ term would have branching fractions below about 3×10^{-17} [8]. Any observation of larger branching fractions would indicate a new source of CP violation in the strong interaction, which could help to solve the problem of the origin of the matter–antimatter asymmetry. The current limit for the $\eta \rightarrow \pi^+\pi^-$ decay mode, $\mathcal{B}(\eta \rightarrow \pi^+\pi^-) < 1.3 \times 10^{-5}$ at 90% confidence level (CL), comes from the KLOE experiment [9], which looked for $\eta \rightarrow \pi^+\pi^-$ in the decay $\phi(1020) \rightarrow \eta\gamma$. The limit for η' , $\mathcal{B}(\eta' \rightarrow \pi^+\pi^-) < 5.5 \times 10^{-5}$ at 90% CL, is from the BESIII experiment [10], based on searches for $\eta' \rightarrow \pi^+\pi^-$ in radiative $J/\psi \rightarrow \eta'\gamma$ decays. In the study presented here, a new method is

introduced to search for the decays $\eta \rightarrow \pi^+\pi^-$ and $\eta' \rightarrow \pi^+\pi^-$, exploiting the large sample of charm mesons collected by LHCb.

2. Detector and simulation

The LHCb detector [11,12] is a single-arm forward spectrometer covering the pseudorapidity range $2 < \eta < 5$, designed for the study of particles containing b or c quarks. The detector includes a high-precision tracking system consisting of a silicon-strip vertex detector surrounding the pp interaction region, a large-area silicon-strip detector located upstream of a dipole magnet with a bending power of about 4 Tm, and three stations of silicon-strip detectors and straw drift tubes placed downstream of the magnet. The tracking system provides a measurement of momentum, p , of charged particles with a relative uncertainty that varies from 0.5% at low momentum to 1.0% at 200 GeV/c. The minimum distance of a track to a primary pp interaction vertex (PV), the impact parameter, is measured with a resolution of $(15 + 29/p_T) \mu\text{m}$, where p_T is the component of the momentum transverse to the beam, in GeV/c. Different types of charged hadrons are distinguished using information from two ring-imaging Cherenkov detectors. Photons, electrons and hadrons are identified by a calorimeter system consisting of scintillating-pad and preshower detectors, an electromagnetic calorimeter and a hadronic calorimeter. Muons are identified by a system composed of alternating layers of iron and multiwire proportional chambers.

The online event selection is performed by a trigger [13], which consists of a hardware stage, based on information from the calorimeter and muon systems, followed by a software stage, which applies a full event reconstruction. At the hardware trigger stage, events are required to have a muon with high p_T or

a hadron, photon or electron with high transverse energy in the calorimeters.

A new scheme for the LHCb software trigger was introduced for LHC Run 2. Alignment and calibration are performed in near real-time [14] and updated constants are made available for the trigger. The same alignment and calibration information is propagated to the offline reconstruction, ensuring high-quality particle identification (PID) and consistent information between the trigger and offline software. The larger timing budget available in the trigger compared to that available in Run 1 also results in the convergence of the online and offline track reconstruction, such that offline performance is achieved in the trigger. The identical performance of the online and offline reconstruction offers the opportunity to perform physics analyses directly using candidates reconstructed in the trigger [15].

In the simulation, pp collisions are generated using PYTHIA [16] with a specific LHCb configuration [17]. Decays of hadronic particles are described by EVTGEN [18], in which final-state radiation is generated using PHOTOS [19]. The interaction of the generated particles with the detector, and its response, are implemented using the GEANT4 toolkit [20] as described in Ref. [21].

3. Data samples and outline of analysis method

In the analysis, the decays $D^+ \rightarrow \pi^+\pi^+\pi^-$ and $D_s^+ \rightarrow \pi^+\pi^+\pi^-$ are used to look for the presence of η and η' resonances in the $\pi^+\pi^-$ mass spectra, which could come from the known decays $D_{(s)}^+ \rightarrow \pi^+\eta^{(\prime)}$ (inclusion of charge-conjugate modes is implied throughout). The data samples comprise about 25 million each of $D^+ \rightarrow \pi^+\pi^+\pi^-$ and $D_s^+ \rightarrow \pi^+\pi^+\pi^-$ decays, from integrated luminosities of 3.0 fb^{-1} of pp collision data recorded by LHCb in LHC Run 1 and 0.3 fb^{-1} recorded in 2015 during Run 2.

For $N(\eta^{(\prime)})$ observed $\eta^{(\prime)}$ signal decays in the $\pi^+\pi^-$ mass spectrum from a total of $N(D_{(s)}^+)$ mesons reconstructed in the $\pi^+\pi^+\pi^-$ final state, the measured branching fraction would be

$$\mathcal{B}(\eta^{(\prime)} \rightarrow \pi^+\pi^-) = \frac{N(\eta^{(\prime)})}{N(D_{(s)}^+)} \times \frac{\mathcal{B}(D_{(s)}^+ \rightarrow \pi^+\pi^+\pi^-)}{\mathcal{B}(D_{(s)}^+ \rightarrow \pi^+\eta^{(\prime)})} \times \frac{1}{\epsilon(\eta^{(\prime)})}, \quad (1)$$

where $\epsilon(\eta^{(\prime)})$ accounts for any variation of efficiency with $\pi^+\pi^-$ mass, as discussed in Sec. 5.2. The values of $N(D_{(s)}^+)$ and $N(\eta^{(\prime)})$ and their uncertainties are obtained from fits to the $\pi^+\pi^-\pi^+$ and $\pi^+\pi^-$ mass spectra of the selected $D_{(s)}^+ \rightarrow \pi^+\pi^+\pi^-$ candidates; the branching fractions $\mathcal{B}(D_{(s)}^+ \rightarrow \pi^+\pi^+\pi^-)$ and $\mathcal{B}(D_{(s)}^+ \rightarrow \pi^+\eta^{(\prime)})$ and their uncertainties are taken from Ref. [22]; and the relative efficiency factors, ϵ , are obtained from simulations. Since the analysis starts from a given number of selected $D_{(s)}^+ \rightarrow \pi^+\pi^+\pi^-$ decays, there are no normalisation channels. All selections are finalised and expected sensitivities are evaluated before the η and η' signal regions in the $\pi^+\pi^-$ mass spectra are examined.

4. Event selection

The event selection comprises an initial stage in which relatively loose criteria are applied to select samples of candidate $D_{(s)}^+ \rightarrow \pi^+\pi^+\pi^-$ decays. A boosted decision tree (BDT) [23] is then used to further suppress backgrounds.

Candidate $D_{(s)}^+ \rightarrow \pi^+\pi^+\pi^-$ decays are required to have three good quality tracks, each with p_T greater than $250 \text{ MeV}/c$, consistent with coming from a vertex that is displaced from any PV in the event. Loose particle identification criteria are applied, requiring the tracks to be consistent with the pion hypothesis. The

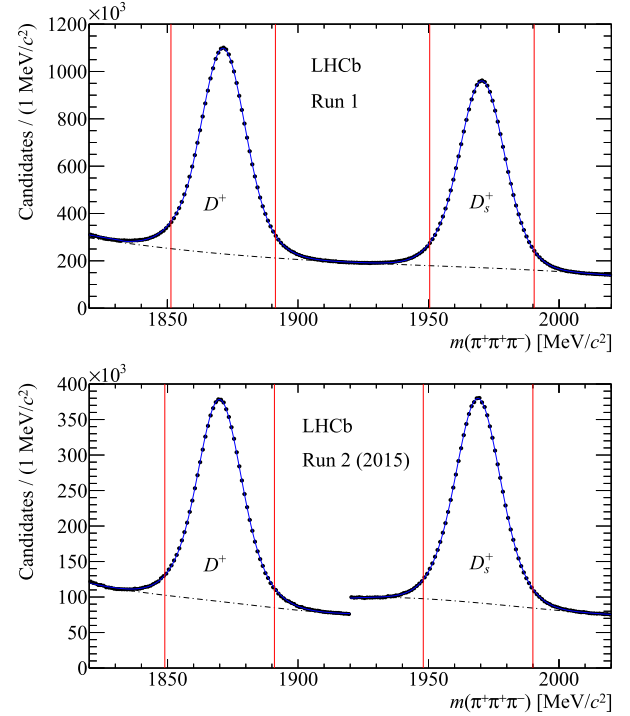


Fig. 1. Mass spectra of selected $D_{(s)}^+ \rightarrow \pi^+\pi^+\pi^-$ candidates, after the BDT selections, for (top) Run 1 and (bottom) Run 2 data, with the results from the fits superimposed. The dot-dashed lines show the total fitted backgrounds, and the vertical lines indicate the optimised $D_{(s)}^+$ signal regions. The discontinuity in the Run 2 spectrum comes from the fact that the trigger has two separate output streams and there are different BDT selections for D^+ and D_s^+ .

three-track system is required to have total charge $\pm e$, its invariant mass must be in the range $1820\text{--}2020 \text{ MeV}/c^2$, and its combined momentum vector must be consistent with the direction from a PV to the decay vertex. The invariant mass of opposite-sign candidate pion pairs is required to be in the range $300\text{--}1650 \text{ MeV}/c^2$; this removes backgrounds where a random pion is associated with a vertex from either a $\gamma \rightarrow e^+e^-$ conversion, in which both electrons are misidentified as pions, or from a $D^0 \rightarrow K^-\pi^+$ decay, where the kaon is misidentified as a pion.

The BDT has six input variables for each of the tracks, together with three variables related to the quality of the decay vertex and the association of the $D_{(s)}^+$ candidate with the PV. The track variables are related to track fit quality, particle identification probabilities and the quality of the track association to the decay vertex. The BDT is trained using a sample of 820 000 simulated $D^+ \rightarrow \pi^+\pi^+\pi^-$ events for the signal, generated uniformly in phase space, and about 10^7 background candidates obtained from sidebands of width $20 \text{ MeV}/c^2$ on each side of the $D^+ \rightarrow \pi^+\pi^+\pi^-$ mass peak in the data.

The selection criteria for the BDT output value and $\pi^+\pi^+\pi^-$ signal mass windows are simultaneously optimised to maximise the statistical significance of the $D_{(s)}^+$ signals, $N_{\text{sig}}/\sqrt{N_{\text{sig}} + N_{\text{bkg}}}$, where N_{sig} is the number of $D_{(s)}^+$ signal decays and N_{bkg} is the number of background events within the signal mass windows. The BDT selection gives signal efficiencies of 90% while rejecting about 60% of the backgrounds. The optimum mass selection ranges are $\pm 20 \text{ MeV}/c^2$ for both the D^+ and D_s^+ peaks in Run 1 and $\pm 21 \text{ MeV}/c^2$ for both peaks in Run 2.

Fig. 1 shows the $\pi^+\pi^+\pi^-$ mass spectra for Runs 1 and 2, after the BDT selection. The discontinuity in the Run 2 spectrum comes from the fact that the trigger has two separate output streams and there are different BDT cuts for D^+ and D_s^+ . The

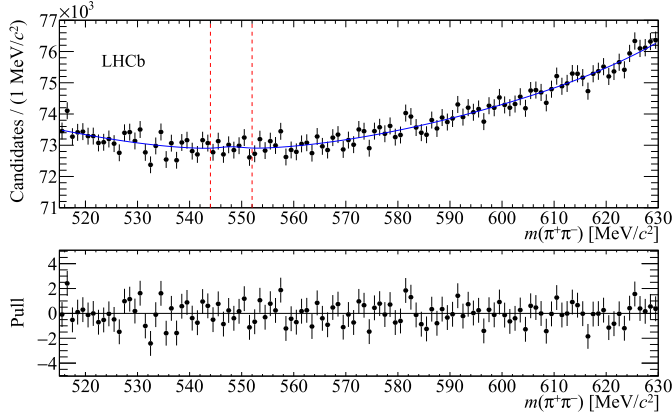


Fig. 2. The $\pi^+\pi^-$ invariant mass distribution in the η mass fitting region from the sum of the four samples, showing also the sum of the fitted curves and the pulls. The vertical dashed lines indicate the η signal region.

yield per fb^{-1} is larger in Run 2 than in Run 1 by a factor 3.3, arising from the larger cross-section [24], and from a higher trigger efficiency for charm. The curves in Fig. 1 show the results of fits to the spectra in which each peak is parametrised by the sum of a double-sided Crystal Ball function [25] and a Gaussian function, while a fourth-order polynomial is used for the combinatorial background. All shape and yield parameters are allowed to vary in the fits. The fits also include components for contributions from $D_s^+ \rightarrow K^+\pi^+\pi^-$ decays, where the kaon is misidentified as a pion, and from $D_s^+ \rightarrow \pi^+\pi^+\pi^-\pi^0$ and $D_{(s)}^+ \rightarrow \pi^+\eta^{(\prime)}$ with $\eta^{(\prime)} \rightarrow \pi^+\pi^-\gamma$. The yields for these last components, the shapes for which are obtained from simulation, are found to be small. The total $D_{(s)}^+ \rightarrow \pi^+\pi^+\pi^-$ signal yields in the optimised mass windows, summed over Run 1 and Run 2 data, are 2.49×10^7 for D^+ and 2.37×10^7 for D_s^+ , with backgrounds of 1.38×10^7 and 1.08×10^7 , respectively, within the same mass windows. Uncertainties of $\pm 2\%$, corresponding to the maximum values of the fit residuals, are assigned to each total yield to account for imperfections in the fits to the mass spectra. To improve the $\pi^+\pi^-$ mass resolution, a kinematic fit [26] is performed on the selected $D_{(s)}^+$ candidates, with the three tracks constrained to a common vertex, the $\pi^+\pi^+\pi^-$ mass constrained to the known $D_{(s)}^+$ mass, and the $D_{(s)}^+$ candidate constrained to come from the PV.

5. Limits on the $\eta^{(\prime)} \rightarrow \pi^+\pi^-$ branching fractions

5.1. Mass spectra for $\pi^+\pi^-$

For each of the η and η' resonances there are four separate $\pi^+\pi^-$ mass spectra, from the D^+ and the D_s^+ for each of Runs 1 and 2. Figs. 2 and 3 show the sums of the four $\pi^+\pi^-$ mass spectra for the η and η' mass fitting ranges, which are chosen to avoid the peaks from the K_S^0 , $\rho(770)^0$ and $f_0(980)$ mesons. The fitting ranges are 515–630 MeV/c^2 for the η and 920–964 MeV/c^2 for the η' . The vertical dashed lines indicate the signal regions, which cover the intervals 544–552 MeV/c^2 for the η and 952–964 MeV/c^2 for the η' , in each case approximately ± 2 times the $\pi^+\pi^-$ mass resolution. Simulation studies of the decays $\eta^{(\prime)} \rightarrow \pi^+\pi^-\gamma$, using the matrix element given in Ref. [27], show that the contributions from these channels are small and do not peak in the fitting ranges. They are therefore considered as part of the background, which is parametrised by a polynomial function (see Sect. 5.3).

Expected signal $\pi^+\pi^-$ mass line shapes for $\eta \rightarrow \pi^+\pi^-$ and $\eta' \rightarrow \pi^+\pi^-$ are obtained from simulations. In both cases a double Gaussian shape is found to describe the signal well, with mass

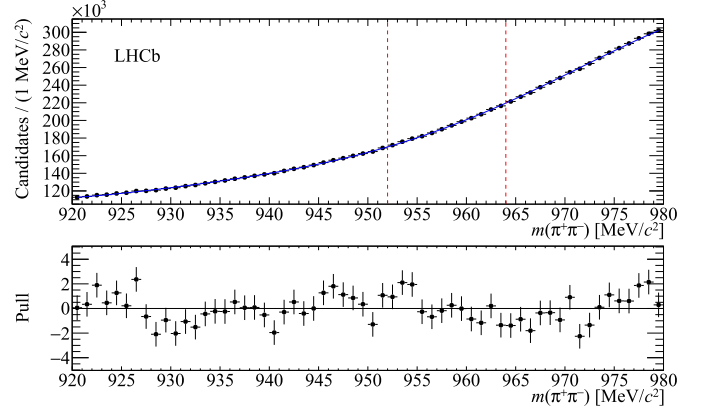


Fig. 3. The $\pi^+\pi^-$ invariant mass distribution in the η' mass fitting region from the sum of the four samples, showing also the sum of the fitted curves and the pulls. The vertical dashed lines indicate the η' signal region.

resolutions of 2.3 MeV/c^2 for the η mass region and 3.2 MeV/c^2 for the η' region. These results are calibrated by comparing the η mass resolution from the simulation with that for reconstructed $K_S^0 \rightarrow \pi^+\pi^-$ decays from background $D_{(s)}^+ \rightarrow K_S^0\pi^+$ events in the data, before the kinematic fits to the $D_{(s)}^+$ candidates. The differences, which are 5% in Run 1 and 10% in Run 2, are taken as the systematic uncertainties on the $\pi^+\pi^-$ mass resolution for both the η and η' mass ranges.

5.2. Relative efficiency as a function of $\pi^+\pi^-$ mass

The relative efficiency factors in Eq. (1) are obtained from simulation. Fully simulated $\pi^+\pi^-$ mass spectra from $D^+ \rightarrow \pi^+\pi^+\pi^-$ decays for Run 1 are divided by the generated spectra to give the relative efficiency as a function of the $\pi^+\pi^-$ mass. The efficiency is highest at large $\pi^+\pi^-$ masses, mainly due to the effects of the hardware and software triggers. The relative efficiencies in Run 1 data are found to be $\epsilon(\eta) = 0.85 \pm 0.01$ and $\epsilon(\eta') = 1.01 \pm 0.01$, where the uncertainties come from the simulation sample size. The relative efficiencies for Run 2 are found to be statistically compatible with those for Run 1, through a comparison of the $\pi^+\pi^-$ mass spectra from the D^+ and D_s^+ signal candidates in the data. An additional systematic uncertainty of 2% is assigned to the Run 2 relative efficiencies, corresponding to the maximum difference between the mass spectra.

5.3. Sensitivity studies

In order to measure the sensitivity of the analysis, each $\pi^+\pi^-$ mass spectrum is fitted with a fourth-order polynomial, initially with the signal regions excluded. The signal regions are then populated with pseudo data, generated according to the fitted polynomial functions, with Gaussian fluctuations. Each spectrum is then fitted again with the sum of a fourth-order polynomial plus the $\eta^{(\prime)}$ signal function, and Eq. (1) is then used to obtain branching fractions measured with the pseudo data. As expected, these branching fractions are consistent with zero. Expected upper limits on the branching fractions are obtained using the CL_s method [28]. In each case, CL_s values are obtained using the products of the likelihood functions for the four individual spectra. Systematic uncertainties are included, but have no effect on the results, which are shown in Fig. 4 for the η and in Fig. 5 for the η' . Expected limits at 90% CL are $\mathcal{B}(\eta \rightarrow \pi^+\pi^-) < 2.0 \times 10^{-5}$ and $\mathcal{B}(\eta' \rightarrow \pi^+\pi^-) < 1.8 \times 10^{-5}$.

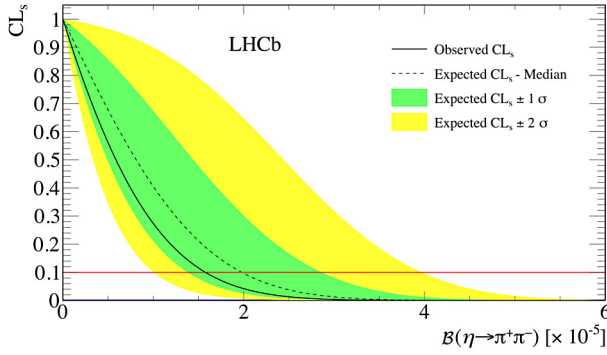


Fig. 4. Values of CL_s as a function of $B(\eta \rightarrow \pi^+\pi^-)$. The expected variation is shown by the dashed line, with the $\pm 1\sigma$ and $\pm 2\sigma$ regions shaded. The observed variation is shown by the solid line, while the horizontal line indicates the 90% confidence level.

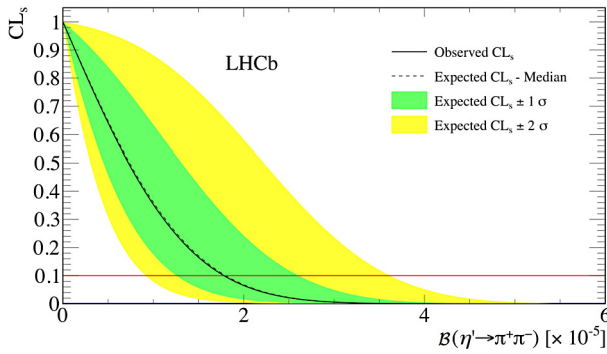


Fig. 5. Values of CL_s as a function of $B(\eta' \rightarrow \pi^+\pi^-)$. The expected variation is shown by the dashed line, with the $\pm 1\sigma$ and $\pm 2\sigma$ regions shaded. The observed variation is shown by the solid line, which almost overlays the dashed line, while the horizontal line indicates the 90% confidence level.

5.4. Observed limits on the branching fractions

The procedures outlined above are then applied to the observed mass spectra, *i.e.* with the pseudo data in the signal ranges replaced by the observed data. The sums of the fits to the four spectra for the η and η' are shown as the solid curves in Figs. 2 and 3. The results are consistent among the four mass spectra for each meson. Weighted average branching fractions are measured to be $B(\eta \rightarrow \pi^+\pi^-) = (-1.1 \pm 1.8) \times 10^{-5}$ and $B(\eta' \rightarrow \pi^+\pi^-) = (0.8 \pm 1.6) \times 10^{-5}$. Although the simple, unweighted sum of the fits to the $\pi^+\pi^-$ mass spectra in Fig. 2 shows a small, but insignificant, positive yield for the η , the weighted average branching fraction $B(\eta \rightarrow \pi^+\pi^-)$ is dominated by a negative value in the Run 1 D_s^+ sample.

Since there is no evidence for any signal, the CL_s method is used, as for the pseudo data, to obtain observed upper limits on the branching fractions. Figs. 4 and 5 show the observed CL_s values as functions of the branching fractions. Limits obtained are

$$B(\eta \rightarrow \pi^+\pi^-) < 1.6 \times 10^{-5},$$

$$B(\eta' \rightarrow \pi^+\pi^-) < 1.8 \times 10^{-5},$$

both at 90% CL, in good agreement with the expected limits.

6. Conclusions

A new method is introduced to search for the decays $\eta \rightarrow \pi^+\pi^-$ and $\eta'(958) \rightarrow \pi^+\pi^-$, which would violate CP symmetry in the strong interaction. The method relies on the copious production of charm mesons at LHCb, and will improve in sensitivity

as more data are collected at the LHC. With the LHC Run 1 data and data from the first year of Run 2, the limit obtained on the branching fraction for the decay $\eta \rightarrow \pi^+\pi^-$ is comparable to the existing limit, while that for $\eta' \rightarrow \pi^+\pi^-$ is a factor three better than the previous limit.

Acknowledgements

We express our gratitude to our colleagues in the CERN accelerator departments for the excellent performance of the LHC. We thank the technical and administrative staff at the LHCb institutes. We acknowledge support from CERN and from the national agencies: CAPES, CNPq, FAPERJ and FINEP (Brazil); NSFC (China); CNRS/IN2P3 (France); BMBF, DFG and MPG (Germany); INFN (Italy); FOM and NWO (The Netherlands); MNiSW and NCN (Poland); MEN/IFA (Romania); MinES and FASO (Russia); MinEco (Spain); SNSF and SER (Switzerland); NASU (Ukraine); STFC (United Kingdom); NSF (USA). We acknowledge the computing resources that are provided by CERN, IN2P3 (France), KIT and DESY (Germany), INFN (Italy), SURF (The Netherlands), PIC (Spain), GridPP (United Kingdom), RRCKI and Yandex LLC (Russia), CSCS (Switzerland), IFIN-HH (Romania), CBPF (Brazil), PL-GRID (Poland) and OSC (USA). We are indebted to the communities behind the multiple open source software packages on which we depend. Individual groups or members have received support from AvH Foundation (Germany), EPLANET, Marie Skłodowska-Curie Actions and ERC (European Union), Conseil Général de Haute-Savoie, Labex ENIGMASS and OCEVU, Région Auvergne (France), RFBR and Yandex LLC (Russia), GVA, XuntaGal and GENCAT (Spain), Herchel Smith Fund, The Royal Society, Royal Commission for the Exhibition of 1851 and the Leverhulme Trust (United Kingdom).

References

- [1] H.-Y. Cheng, The strong CP problem revisited, *Phys. Rep.* 158 (1988) 1.
- [2] J. Kukei, et al., Strong CP violation and the neutron electric dipole form factor, *Phys. At. Nucl.* 70 (2007) 349, arXiv:hep-ph/0510116.
- [3] R.D. Peccei, The strong CP problem and axions, *Lect. Notes Phys.* 741 (2008) 3, arXiv:hep-ph/0607268.
- [4] S.Yu. Khlebnikov, M.E. Shaposhnikov, Extra space–time dimensions: towards a solution to the strong CP problem, *Phys. Lett. B* 203 (1988) 121.
- [5] D.R. Nelson, G.T. Fleming, G.W. Kilcup, Up quark mass in lattice QCD with three light dynamical quarks and implications for strong CP invariance, *Phys. Rev. Lett.* 90 (2003) 021601, arXiv:hep-lat/0112029.
- [6] R.G. Leigh, The strong CP problem, string theory and the Nelson–Barr mechanism, in: J.L. Lopez, D.V. Nanopoulos (Eds.), *Recent Advances in the Superworld*, World Scientific, 1994, arXiv:hep-ph/9307214.
- [7] Z.G. Berezhiani, R.N. Mohapatra, G. Senjanovic, Planck-scale physics and solutions to the strong CP problem without the axion, *Phys. Rev. D* 47 (1993) 5565, arXiv:hep-ph/9212318.
- [8] C. Jarlskog, E. Shabalin, How large are the rates of the CP violating $\eta, \eta' \rightarrow \pi\pi$ decays?, *Phys. Rev. D* 52 (1995) 248.
- [9] KLOE collaboration, F. Ambrosino, et al., Upper limit on the $\eta \rightarrow \pi^+\pi^-$ branching ratio with the KLOE detector, *Phys. Lett. B* 606 (2005) 276, arXiv:hep-ex/0411030.
- [10] BESIII collaboration, M. Ablikim, et al., Search for CP and P violating pseudoscalar decays into $\pi\pi$, *Phys. Rev. D* 84 (2011) 032006, arXiv:1106.5118.
- [11] LHCb collaboration, A.A. Alves Jr, et al., The LHCb detector at the LHC, *J. Instrum.* 3 (2008) S08005.
- [12] LHCb collaboration, R. Aaij, et al., LHCb detector performance, *Int. J. Mod. Phys. A* 30 (2015) 1530022, arXiv:1412.6352.
- [13] R. Aaij, et al., The LHCb trigger and its performance in 2011, *J. Instrum.* 8 (2013) P04022, arXiv:1211.3055.
- [14] G. Dujany, B. Storaci, Real-time alignment and calibration of the LHCb detector in Run II, *J. Phys. Conf. Ser.* 664 (2015) 082010.
- [15] S. Benson, V. Gligorov, M.A. Vesterinen, J.M. Williams, The LHCb turbo stream, *J. Phys. Conf. Ser.* 664 (2015) 082004.
- [16] T. Sjöstrand, S. Mrenna, P. Skands, PYTHIA 6.4 physics and manual, *J. High Energy Phys.* 05 (2006) 026, arXiv:hep-ph/0603175; T. Sjöstrand, S. Mrenna, P. Skands, A brief introduction to PYTHIA 8.1, *Comput. Phys. Commun.* 178 (2008) 852, arXiv:0710.3820.

- [17] I. Belyaev, et al., Handling of the generation of primary events in Gauss, the LHCb simulation framework, *J. Phys. Conf. Ser.* 331 (2011) 032047.
- [18] D.J. Lange, The EvtGen particle decay simulation package, *Nucl. Instrum. Methods A* 462 (2001) 152.
- [19] P. Golonka, Z. Was, PHOTOS Monte Carlo: a precision tool for QED corrections in Z and W decays, *Eur. Phys. J. C* 45 (2006) 97, arXiv:hep-ph/0506026.
- [20] Geant4 collaboration, J. Allison, et al., Geant4 developments and applications, *IEEE Trans. Nucl. Sci.* 53 (2006) 270; Geant4 collaboration, S. Agostinelli, et al., Geant4: a simulation toolkit, *Nucl. Instrum. Methods A* 506 (2003) 250.
- [21] M. Clemencic, et al., The LHCb simulation application, Gauss: design, evolution and experience, *J. Phys. Conf. Ser.* 331 (2011) 032023.
- [22] Particle Data Group, K.A. Olive, et al., Review of particle physics, *Chin. Phys. C* 38 (2014) 090001, and 2015 update.
- [23] B.P. Roe, et al., Boosted decision trees as an alternative to artificial neural networks for particle identification, *Nucl. Instrum. Methods A* 543 (2005) 577, arXiv:physics/0408124.
- [24] LHCb collaboration, R. Aaij, et al., Measurements of prompt charm production cross-sections in pp collisions at $\sqrt{s} = 13$ TeV, *J. High Energy Phys.* 03 (2016) 159, arXiv:1510.01707.
- [25] T. Skwarnicki, A Study of the Radiative CASCADE Transitions Between the Upsilon-Prime and Upsilon Resonances, PhD thesis, Institute of Nuclear Physics, Krakow, 1986, DESY-F31-86-02.
- [26] W.D. Hulsbergen, Decay chain fitting with a Kalman filter, *Nucl. Instrum. Methods A* 552 (2005) 566, arXiv:physics/0503191.
- [27] WASA-at-COSY collaboration, P. Adlarson, et al., Exclusive measurement of the $\eta \rightarrow \pi^+\pi^-\gamma$ decay, *Phys. Lett. B* 707 (2012) 243, arXiv:1107.5277.
- [28] A.L. Read, Presentation of search results: the CL_s technique, *J. Phys. G, Nucl. Part. Phys.* 28 (2002) 2693.

The LHCb Collaboration

R. Aaij⁴⁰, B. Adeva³⁹, M. Adinolfi⁴⁸, Z. Ajaltouni⁵, S. Akar⁶, J. Albrecht¹⁰, F. Alessio⁴⁰, M. Alexander⁵³, S. Ali⁴³, G. Alkhazov³¹, P. Alvarez Cartelle⁵⁵, A.A. Alves Jr⁵⁹, S. Amato², S. Amerio²³, Y. Amhis⁷, L. An⁴¹, L. Anderlini¹⁸, G. Andreassi⁴¹, M. Andreotti^{17,g}, J.E. Andrews⁶⁰, R.B. Appleby⁵⁶, F. Archilli⁴³, P. d'Argent¹², J. Arnau Romeu⁶, A. Artamonov³⁷, M. Artuso⁶¹, E. Aslanides⁶, G. Auriemma²⁶, M. Baalouch⁵, I. Babuschkin⁵⁶, S. Bachmann¹², J.J. Back⁵⁰, A. Badalov³⁸, C. Baesso⁶², S. Baker⁵⁵, W. Baldini¹⁷, R.J. Barlow⁵⁶, C. Barschel⁴⁰, S. Barsuk⁷, W. Barter⁴⁰, M. Baszczyk²⁷, V. Batozskaya²⁹, B. Batsukh⁶¹, V. Battista⁴¹, A. Bay⁴¹, L. Beaucourt⁴, J. Beddow⁵³, F. Bedeschi²⁴, I. Bediaga¹, L.J. Bel⁴³, V. Bellee⁴¹, N. Belloli^{21,i}, K. Belous³⁷, I. Belyaev³², E. Ben-Haim⁸, G. Bencivenni¹⁹, S. Benson⁴³, J. Benton⁴⁸, A. Berezhnoy³³, R. Bernet⁴², A. Bertolin²³, C. Betancourt⁴², F. Betti¹⁵, M.-O. Bettler⁴⁰, M. van Beuzekom⁴³, Ia. Bezshyiko⁴², S. Bifani⁴⁷, P. Billoir⁸, T. Bird⁵⁶, A. Birnkraut¹⁰, A. Bitadze⁵⁶, A. Bizzeti^{18,u}, T. Blake⁵⁰, F. Blanc⁴¹, J. Blouw^{11,t}, S. Blusk⁶¹, V. Bocci²⁶, T. Boettcher⁵⁸, A. Bondar^{36,w}, N. Bondar^{31,40}, W. Bonivento¹⁶, I. Bordyuzhin³², A. Borgheresi^{21,i}, S. Borghi⁵⁶, M. Borisyak³⁵, M. Borsato³⁹, F. Bossu⁷, M. Boubdir⁹, T.J.V. Bowcock⁵⁴, E. Bowen⁴², C. Bozzi^{17,40}, S. Braun¹², M. Britsch¹², T. Britton⁶¹, J. Brodzicka⁵⁶, E. Buchanan⁴⁸, C. Burr⁵⁶, A. Bursche², J. Buytaert⁴⁰, S. Cadeddu¹⁶, R. Calabrese^{17,g}, M. Calvi^{21,i}, M. Calvo Gomez^{38,m}, A. Camboni³⁸, P. Campana¹⁹, D.H. Campora Perez⁴⁰, L. Capriotti^{56,*}, A. Carbone^{15,e}, G. Carboni^{25,j}, R. Cardinale^{20,h}, A. Cardini¹⁶, P. Carniti^{21,i}, L. Carson⁵², K. Carvalho Akiba², G. Casse⁵⁴, L. Cassina^{21,i}, L. Castillo Garcia⁴¹, M. Cattaneo⁴⁰, Ch. Cauet¹⁰, G. Cavallero²⁰, R. Cenci^{24,t}, D. Chamont⁷, M. Charles⁸, Ph. Charpentier⁴⁰, G. Chatzikonstantinidis⁴⁷, M. Chefdeville⁴, S. Chen⁵⁶, S.-F. Cheung⁵⁷, V. Chobanova³⁹, M. Chrzaszcz^{42,27}, X. Cid Vidal³⁹, G. Ciezarek⁴³, P.E.L. Clarke⁵², M. Clemencic⁴⁰, H.V. Cliff⁴⁹, J. Closier⁴⁰, V. Coco⁵⁹, J. Cogan⁶, E. Cogneras⁵, V. Cogoni^{16,40,f}, L. Cojocariu³⁰, G. Collazuol^{23,o}, P. Collins⁴⁰, A. Comerma-Montells¹², A. Contu⁴⁰, A. Cook⁴⁸, G. Coombs⁴⁰, S. Coquereau³⁸, G. Corti⁴⁰, M. Corvo^{17,g}, C.M. Costa Sobral⁵⁰, B. Couturier⁴⁰, G.A. Cowan⁵², D.C. Craik⁵², A. Crocombe⁵⁰, M. Cruz Torres⁶², S. Cunliffe⁵⁵, R. Currie⁵⁵, C. D'Ambrosio⁴⁰, F. Da Cunha Marinho², E. Dall'Occo⁴³, J. Dalseno⁴⁸, P.N.Y. David⁴³, A. Davis⁵⁹, O. De Aguiar Francisco², K. De Bruyn⁶, S. De Capua⁵⁶, M. De Cian¹², J.M. De Miranda¹, L. De Paula², M. De Serio^{14,d}, P. De Simone¹⁹, C.-T. Dean⁵³, D. Decamp⁴, M. Deckenhoff¹⁰, L. Del Buono⁸, M. Demmer¹⁰, A. Dendek²⁸, D. Derkach³⁵, O. Deschamps⁵, F. Dettori⁴⁰, B. Dey²², A. Di Canto⁴⁰, H. Dijkstra⁴⁰, F. Dordei⁴⁰, M. Dorigo⁴¹, A. Dosil Suárez³⁹, A. Dovbnya⁴⁵, K. Dreimanis⁵⁴, L. Dufour⁴³, G. Dujany⁵⁶, K. Dungs⁴⁰, P. Durante⁴⁰, R. Dzhelezhadine³⁷, A. Dziurda⁴⁰, A. Dzyuba³¹, N. Déléage⁴, S. Easo⁵¹, M. Ebert⁵², U. Egede⁵⁵, V. Egorychev³², S. Eidelman^{36,w}, S. Eisenhardt⁵², U. Eitschberger¹⁰, R. Ekelhof¹⁰, L. Eklund⁵³, S. Ely⁶¹, S. Esen¹², H.M. Evans⁴⁹, T. Evans⁵⁷, A. Falabella¹⁵, N. Farley⁴⁷, S. Farry⁵⁴, R. Fay⁵⁴, D. Fazzini^{21,i}, D. Ferguson⁵², A. Fernandez Prieto³⁹, F. Ferrari^{15,40}, F. Ferreira Rodrigues², M. Ferro-Luzzi⁴⁰, S. Filippov³⁴, R.A. Fini¹⁴, M. Fiore^{17,g}, M. Fiorini^{17,g}, M. Firlej²⁸, C. Fitzpatrick⁴¹, T. Fiutowski²⁸, F. Fleuret^{7,b}, K. Fohl⁴⁰, M. Fontana^{16,40}, F. Fontanelli^{20,h}, D.C. Forshaw⁶¹, R. Forty⁴⁰, V. Franco Lima⁵⁴, M. Frank⁴⁰, C. Frei⁴⁰, J. Fu^{22,q}, E. Furfaro^{25,j}, C. Färber⁴⁰, A. Gallas Torreira³⁹, D. Galli^{15,e}, S. Gallorini²³, S. Gambetta⁵², M. Gandelman², P. Gandini⁵⁷, Y. Gao³, L.M. Garcia Martin⁶⁸, J. García Pardiñas³⁹, J. Garra Tico⁴⁹, L. Garrido³⁸, P.J. Garsed⁴⁹, D. Gascon³⁸, C. Gaspar⁴⁰, L. Gavardi¹⁰, G. Gazzoni⁵, D. Gerick¹², E. Gersabeck¹², M. Gersabeck⁵⁶, T. Gershon⁵⁰, Ph. Ghez⁴, S. Gianì⁴¹, V. Gibson⁴⁹,

O.G. Girard⁴¹, L. Giubega³⁰, K. Gizdov⁵², V.V. Gligorov⁸, D. Golubkov³², A. Golutvin^{55,40}, A. Gomes^{1,a}, I.V. Gorelov³³, C. Gotti^{21,i}, M. Grabalosa Gándara⁵, R. Graciani Diaz³⁸, L.A. Granado Cardoso⁴⁰, E. Graugés³⁸, E. Graverini⁴², G. Graziani¹⁸, A. Grecu³⁰, P. Griffith⁴⁷, L. Grillo^{21,40,i}, B.R. Gruberg Cazon⁵⁷, O. Grünberg⁶⁶, E. Gushchin³⁴, Yu. Guz³⁷, T. Gys⁴⁰, C. Göbel⁶², T. Hadavizadeh⁵⁷, C. Hadjivasiliou⁵, G. Haefeli⁴¹, C. Haen⁴⁰, S.C. Haines⁴⁹, S. Hall⁵⁵, B. Hamilton⁶⁰, X. Han¹², S. Hansmann-Menzemer¹², N. Harnew⁵⁷, S.T. Harnew⁴⁸, J. Harrison⁵⁶, M. Hatch⁴⁰, J. He⁶³, T. Head⁴¹, A. Heister⁹, K. Hennessy⁵⁴, P. Henrard⁵, L. Henry⁸, J.A. Hernando Morata³⁹, E. van Herwijnen⁴⁰, M. Heß⁶⁶, A. Hicheur², D. Hill⁵⁷, C. Hombach⁵⁶, H. Hopchev⁴¹, W. Hulsbergen⁴³, T. Humair⁵⁵, M. Hushchyn³⁵, N. Hussain⁵⁷, D. Hutchcroft⁵⁴, M. Idzik²⁸, P. Ilten⁵⁸, R. Jacobsson⁴⁰, A. Jaeger¹², J. Jalocha⁵⁷, E. Jans⁴³, A. Jawahery⁶⁰, F. Jiang³, M. John⁵⁷, D. Johnson⁴⁰, C.R. Jones⁴⁹, C. Joram⁴⁰, B. Jost⁴⁰, N. Jurik⁶¹, S. Kandybei⁴⁵, W. Kanso⁶, M. Karacson⁴⁰, J.M. Kariuki⁴⁸, S. Karodia⁵³, M. Kecke¹², M. Kelsey⁶¹, I.R. Kenyon⁴⁷, M. Kenzie⁴⁹, T. Ketel⁴⁴, E. Khairullin³⁵, B. Khanji¹², C. Khurewathanakul⁴¹, T. Kirn⁹, S. Klaver⁵⁶, K. Klimaszewski²⁹, S. Koliiev⁴⁶, M. Kolpin¹², I. Komarov⁴¹, R.F. Koopman⁴⁴, P. Koppenburg⁴³, A. Kosmyntseva³², A. Kozachuk³³, M. Kozeiha⁵, L. Kravchuk³⁴, K. Kreplin¹², M. Kreps⁵⁰, P. Krokovny^{36,w}, F. Kruse¹⁰, W. Krzemien²⁹, W. Kucewicz^{27,l}, M. Kucharczyk²⁷, V. Kudryavtsev^{36,w}, A.K. Kuonen⁴¹, K. Kurek²⁹, T. Kvaratskheliya^{32,40}, D. Lacarrere⁴⁰, G. Lafferty⁵⁶, A. Lai¹⁶, G. Lanfranchi¹⁹, C. Langenbruch⁹, T. Latham⁵⁰, C. Lazzeroni⁴⁷, R. Le Gac⁶, J. van Leerdam⁴³, J.-P. Lees⁴, A. Leflat^{33,40}, J. Lefrançois⁷, R. Lefèvre⁵, F. Lemaître⁴⁰, E. Lemos Cid³⁹, O. Leroy⁶, T. Lesiak²⁷, B. Leverington¹², T. Li³, Y. Li⁷, T. Likhomanenko^{35,67}, R. Lindner⁴⁰, C. Linn⁴⁰, F. Lionetto⁴², B. Liu¹⁶, X. Liu³, D. Loh⁵⁰, I. Longstaff⁵³, J.H. Lopes², D. Lucchesi^{23,o}, M. Lucio Martinez³⁹, H. Luo⁵², A. Lupato²³, E. Luppi^{17,g}, O. Lupton⁵⁷, A. Lusiani²⁴, X. Lyu⁶³, F. Machefert⁷, F. Maciuc³⁰, O. Maev³¹, K. Maguire⁵⁶, S. Malde⁵⁷, A. Malinin⁶⁷, T. Maltsev³⁶, G. Manca⁷, G. Mancinelli⁶, P. Manning⁶¹, J. Maratas^{5,v}, J.F. Marchand⁴, U. Marconi¹⁵, C. Marin Benito³⁸, P. Marino^{24,t}, J. Marks¹², G. Martellotti²⁶, M. Martin⁶, M. Martinelli⁴¹, D. Martinez Santos³⁹, F. Martinez Vidal⁶⁸, D. Martins Tostes², L.M. Massacrier⁷, A. Massafferri¹, R. Matev⁴⁰, A. Mathad⁵⁰, Z. Mathe⁴⁰, C. Matteuzzi²¹, A. Mauri⁴², B. Maurin⁴¹, A. Mazurov⁴⁷, M. McCann⁵⁵, J. McCarthy⁴⁷, A. McNab⁵⁶, R. McNulty¹³, B. Meadows⁵⁹, F. Meier¹⁰, M. Meissner¹², D. Melnychuk²⁹, M. Merk⁴³, A. Merli^{22,q}, E. Michielin²³, D.A. Milanes⁶⁵, M.-N. Minard⁴, D.S. Mitzel¹², A. Mogini⁸, J. Molina Rodriguez¹, I.A. Monroy⁶⁵, S. Monteil⁵, M. Morandin²³, P. Morawski²⁸, A. Mordà⁶, M.J. Morello^{24,t}, J. Moron²⁸, A.B. Morris⁵², R. Mountain⁶¹, F. Muheim⁵², M. Mulder⁴³, M. Mussini¹⁵, D. Müller⁵⁶, J. Müller¹⁰, K. Müller⁴², V. Müller¹⁰, P. Naik⁴⁸, T. Nakada⁴¹, R. Nandakumar⁵¹, A. Nandi⁵⁷, I. Nasteva², M. Needham⁵², N. Neri²², S. Neubert¹², N. Neufeld⁴⁰, M. Neuner¹², A.D. Nguyen⁴¹, T.D. Nguyen⁴¹, C. Nguyen-Mau^{41,n}, S. Nieswand⁹, R. Niet¹⁰, N. Nikitin³³, T. Nikodem¹², A. Novoselov³⁷, D.P. O'Hanlon⁵⁰, A. Oblakowska-Mucha²⁸, V. Obraztsov³⁷, S. Ogilvy¹⁹, R. Oldeman⁴⁹, C.J.G. Onderwater⁶⁹, J.M. Otalora Goicochea², A. Otto⁴⁰, P. Owen⁴², A. Oyanguren^{68,40}, P.R. Pais⁴¹, A. Palano^{14,d}, F. Palombo^{22,q}, M. Palutan¹⁹, J. Panman⁴⁰, A. Papanestis⁵¹, M. Pappagallo^{14,d}, L.L. Pappalardo^{17,g}, W. Parker⁶⁰, C. Parkes⁵⁶, G. Passaleva¹⁸, A. Pastore^{14,d}, G.D. Patel⁵⁴, M. Patel⁵⁵, C. Patrignani^{15,e}, A. Pearce^{56,51}, A. Pellegrino⁴³, G. Penso²⁶, M. Pepe Altarelli⁴⁰, S. Perazzini⁴⁰, P. Perret⁵, L. Pescatore⁴⁷, K. Petridis⁴⁸, A. Petrolini^{20,h}, A. Petrov⁶⁷, M. Petruzzo^{22,q}, E. Picatoste Olloqui³⁸, B. Pietrzyk⁴, M. Pikiés²⁷, D. Pinci²⁶, A. Pistone²⁰, A. Piucci¹², S. Playfer⁵², M. Plo Casasus³⁹, T. Poikela⁴⁰, F. Polci⁸, A. Poluektov^{50,36}, I. Polyakov⁶¹, E. Polcarpo², G.J. Pomery⁴⁸, A. Popov³⁷, D. Popov^{11,40}, B. Popovici³⁰, S. Poslavskii³⁷, C. Potterat², E. Price⁴⁸, J.D. Price⁵⁴, J. Prisciandaro³⁹, A. Pritchard⁵⁴, C. Prouve⁴⁸, V. Pugatch⁴⁶, A. Puig Navarro⁴¹, G. Punzi^{24,p}, W. Qian⁵⁷, R. Quagliani^{7,48}, B. Rachwal²⁷, J.H. Rademacker⁴⁸, M. Rama²⁴, M. Ramos Pernas³⁹, M.S. Rangel², I. Raniuk⁴⁵, F. Ratnikov³⁵, G. Raven⁴⁴, F. Redi⁵⁵, S. Reichert¹⁰, A.C. dos Reis¹, C. Remon Alepuz⁶⁸, V. Renaudin⁷, S. Ricciardi⁵¹, S. Richards⁴⁸, M. Rihl⁴⁰, K. Rinnert⁵⁴, V. Rives Molina³⁸, P. Robbe^{7,40}, A.B. Rodrigues¹, E. Rodrigues⁵⁹, J.A. Rodriguez Lopez⁶⁵, P. Rodriguez Perez^{56,†}, A. Rogozhnikov³⁵, S. Roiser⁴⁰, A. Rollings⁵⁷, V. Romanovskiy³⁷, A. Romero Vidal³⁹, J.W. Ronayne¹³, M. Rotondo¹⁹, M.S. Rudolph⁶¹, T. Ruf⁴⁰, P. Ruiz Valls⁶⁸, J.J. Saborido Silva³⁹, E. Sadykhov³², N. Sagidova³¹, B. Saitta^{16,f}, V. Salustino Guimaraes², C. Sanchez Mayordomo⁶⁸, B. Sanmartin Sedes³⁹, R. Santacesaria²⁶, C. Santamarina Rios³⁹, M. Santimaria¹⁹, E. Santovetti^{25,j}, A. Sarti^{19,k}, C. Satriano^{26,s}, A. Satta²⁵, D.M. Saunders⁴⁸, D. Savrina^{32,33}, S. Schael⁹, M. Schellenberg¹⁰, M. Schiller⁴⁰,

H. Schindler⁴⁰, M. Schlupp¹⁰, M. Schmelling¹¹, T. Schmelzer¹⁰, B. Schmidt⁴⁰, O. Schneider⁴¹, A. Schopper⁴⁰, K. Schubert¹⁰, M. Schubiger⁴¹, M.-H. Schune⁷, R. Schwemmer⁴⁰, B. Sciascia¹⁹, A. Sciubba^{26,k}, A. Semennikov³², A. Sergi⁴⁷, N. Serra⁴², J. Serrano⁶, L. Sestini²³, P. Seyfert²¹, M. Shapkin³⁷, I. Shapoval⁴⁵, Y. Shcheglov³¹, T. Shears⁵⁴, L. Shekhtman^{36,w}, V. Shevchenko⁶⁷, B.G. Siddi^{17,40}, R. Silva Coutinho⁴², L. Silva de Oliveira², G. Simi^{23,o}, S. Simone^{14,d}, M. Sirendi⁴⁹, N. Skidmore⁴⁸, T. Skwarnicki⁶¹, E. Smith⁵⁵, I.T. Smith⁵², J. Smith⁴⁹, M. Smith⁵⁵, H. Snoek⁴³, M.D. Sokoloff⁵⁹, F.J.P. Soler⁵³, B. Souza De Paula², B. Spaan¹⁰, P. Spradlin⁵³, S. Sridharan⁴⁰, F. Stagni⁴⁰, M. Stahl¹², S. Stahl⁴⁰, P. Stefko⁴¹, S. Stefkova⁵⁵, O. Steinkamp⁴², S. Stemmle¹², O. Stenyakin³⁷, S. Stevenson⁵⁷, S. Stoica³⁰, S. Stone⁶¹, B. Storaci⁴², S. Stracka^{24,p}, M. Straticiu³⁰, U. Straumann⁴², L. Sun⁵⁹, W. Sutcliffe⁵⁵, K. Swientek²⁸, V. Syropoulos⁴⁴, M. Szczekowski²⁹, T. Szumlak²⁸, S. T'Jampens⁴, A. Tayduganov⁶, T. Tekampe¹⁰, G. Tellarini^{17,g}, F. Teubert⁴⁰, E. Thomas⁴⁰, J. van Tilburg⁴³, M.J. Tilley⁵⁵, V. Tisserand⁴, M. Tobin⁴¹, S. Tolk⁴⁹, L. Tomassetti^{17,g}, D. Tonelli⁴⁰, S. Topp-Joergensen⁵⁷, F. Toriello⁶¹, E. Tournefier⁴, S. Tourneur⁴¹, K. Trabelsi⁴¹, M. Traill⁵³, M.T. Tran⁴¹, M. Tresch⁴², A. Trisovic⁴⁰, A. Tsaregorodtsev⁶, P. Tsopelas⁴³, A. Tully⁴⁹, N. Tuning⁴³, A. Ukleja²⁹, A. Ustyuzhanin³⁵, U. Uwer¹², C. Vacca^{16,f}, V. Vagnoni^{15,40}, A. Valassi⁴⁰, S. Valat⁴⁰, G. Valenti¹⁵, A. Vallier⁷, R. Vazquez Gomez¹⁹, P. Vazquez Regueiro³⁹, S. Vecchi¹⁷, M. van Veghel⁴³, J.J. Velthuis⁴⁸, M. Veltri^{18,r}, G. Veneziano⁵⁷, A. Venkateswaran⁶¹, M. Vernet⁵, M. Vesterinen¹², B. Viaud⁷, D. Vieira¹, M. Vieites Diaz³⁹, H. Viemann⁶⁶, X. Vilasis-Cardona^{38,m}, M. Vitti⁴⁹, V. Volkov³³, A. Vollhardt⁴², B. Voneki⁴⁰, A. Vorobyev³¹, V. Vorobyev^{36,w}, C. Voß⁶⁶, J.A. de Vries⁴³, C. Vázquez Sierra³⁹, R. Waldi⁶⁶, C. Wallace⁵⁰, R. Wallace¹³, J. Walsh²⁴, J. Wang⁶¹, D.R. Ward⁴⁹, H.M. Wark⁵⁴, N.K. Watson⁴⁷, D. Websdale⁵⁵, A. Weiden⁴², M. Whitehead⁴⁰, J. Wicht⁵⁰, G. Wilkinson^{57,40}, M. Wilkinson⁶¹, M. Williams⁴⁰, M.P. Williams⁴⁷, M. Williams⁵⁸, T. Williams⁴⁷, F.F. Wilson⁵¹, J. Wimberley⁶⁰, J. Wishahi¹⁰, W. Wislicki²⁹, M. Witek²⁷, G. Wormser⁷, S.A. Wotton⁴⁹, K. Wraight⁵³, K. Wyllie⁴⁰, Y. Xie⁶⁴, Z. Xing⁶¹, Z. Xu⁴¹, Z. Yang³, Y. Yao⁶¹, H. Yin⁶⁴, J. Yu⁶⁴, X. Yuan^{36,w}, O. Yushchenko³⁷, K.A. Zarebski⁴⁷, M. Zavertyaev^{11,c}, L. Zhang³, Y. Zhang⁷, Y. Zhang⁶³, A. Zhelezov¹², Y. Zheng⁶³, A. Zhokhov³², X. Zhu³, V. Zhukov⁹, S. Zucchelli¹⁵

¹ Centro Brasileiro de Pesquisas Físicas (CBPF), Rio de Janeiro, Brazil

² Universidade Federal do Rio de Janeiro (UFRJ), Rio de Janeiro, Brazil

³ Center for High Energy Physics, Tsinghua University, Beijing, China

⁴ LAPP, Université Savoie Mont-Blanc, CNRS/IN2P3, Annecy-Le-Vieux, France

⁵ Clermont Université, Université Blaise Pascal, CNRS/IN2P3, LPC, Clermont-Ferrand, France

⁶ CPPM, Aix-Marseille Université, CNRS/IN2P3, Marseille, France

⁷ LAL, Université Paris-Sud, CNRS/IN2P3, Orsay, France

⁸ LPNHE, Université Pierre et Marie Curie, Université Paris Diderot, CNRS/IN2P3, Paris, France

⁹ I. Physikalisches Institut, RWTH Aachen University, Aachen, Germany

¹⁰ Fakultät Physik, Technische Universität Dortmund, Dortmund, Germany

¹¹ Max-Planck-Institut für Kernphysik (MPIK), Heidelberg, Germany

¹² Physikalisches Institut, Ruprecht-Karls-Universität Heidelberg, Heidelberg, Germany

¹³ School of Physics, University College Dublin, Dublin, Ireland

¹⁴ Sezione INFN di Bari, Bari, Italy

¹⁵ Sezione INFN di Bologna, Bologna, Italy

¹⁶ Sezione INFN di Cagliari, Cagliari, Italy

¹⁷ Sezione INFN di Ferrara, Ferrara, Italy

¹⁸ Sezione INFN di Firenze, Firenze, Italy

¹⁹ Laboratori Nazionali dell'INFN di Frascati, Frascati, Italy

²⁰ Sezione INFN di Genova, Genova, Italy

²¹ Sezione INFN di Milano Bicocca, Milano, Italy

²² Sezione INFN di Milano, Milano, Italy

²³ Sezione INFN di Padova, Padova, Italy

²⁴ Sezione INFN di Pisa, Pisa, Italy

²⁵ Sezione INFN di Roma Tor Vergata, Roma, Italy

²⁶ Sezione INFN di Roma La Sapienza, Roma, Italy

²⁷ Henryk Niewodniczanski Institute of Nuclear Physics Polish Academy of Sciences, Kraków, Poland

²⁸ AGH – University of Science and Technology, Faculty of Physics and Applied Computer Science, Kraków, Poland

²⁹ National Center for Nuclear Research (NCBJ), Warsaw, Poland

³⁰ Horia Hulubei National Institute of Physics and Nuclear Engineering, Bucharest-Magurele, Romania

³¹ Petersburg Nuclear Physics Institute (PNPI), Gatchina, Russia

³² Institute of Theoretical and Experimental Physics (ITEP), Moscow, Russia

³³ Institute of Nuclear Physics, Moscow State University (SINP MSU), Moscow, Russia

³⁴ Institute for Nuclear Research of the Russian Academy of Sciences (INR RAN), Moscow, Russia

³⁵ Yandex School of Data Analysis, Moscow, Russia

³⁶ Budker Institute of Nuclear Physics (SB RAS), Novosibirsk, Russia

³⁷ Institute for High Energy Physics (IHEP), Protvino, Russia

³⁸ ICCUB, Universitat de Barcelona, Barcelona, Spain

³⁹ Universidad de Santiago de Compostela, Santiago de Compostela, Spain

- ⁴⁰ European Organization for Nuclear Research (CERN), Geneva, Switzerland
⁴¹ Ecole Polytechnique Fédérale de Lausanne (EPFL), Lausanne, Switzerland
⁴² Physik-Institut, Universität Zürich, Zürich, Switzerland
⁴³ Nikhef National Institute for Subatomic Physics, Amsterdam, The Netherlands
⁴⁴ Nikhef National Institute for Subatomic Physics and VU University Amsterdam, Amsterdam, The Netherlands
⁴⁵ NSC Kharkiv Institute of Physics and Technology (NSC KIPT), Kharkiv, Ukraine
⁴⁶ Institute for Nuclear Research of the National Academy of Sciences (KINR), Kyiv, Ukraine
⁴⁷ University of Birmingham, Birmingham, United Kingdom
⁴⁸ H.H. Wills Physics Laboratory, University of Bristol, Bristol, United Kingdom
⁴⁹ Cavendish Laboratory, University of Cambridge, Cambridge, United Kingdom
⁵⁰ Department of Physics, University of Warwick, Coventry, United Kingdom
⁵¹ STFC Rutherford Appleton Laboratory, Didcot, United Kingdom
⁵² School of Physics and Astronomy, University of Edinburgh, Edinburgh, United Kingdom
⁵³ School of Physics and Astronomy, University of Glasgow, Glasgow, United Kingdom
⁵⁴ Oliver Lodge Laboratory, University of Liverpool, Liverpool, United Kingdom
⁵⁵ Imperial College London, London, United Kingdom
⁵⁶ School of Physics and Astronomy, University of Manchester, Manchester, United Kingdom
⁵⁷ Department of Physics, University of Oxford, Oxford, United Kingdom
⁵⁸ Massachusetts Institute of Technology, Cambridge, MA, United States
⁵⁹ University of Cincinnati, Cincinnati, OH, United States
⁶⁰ University of Maryland, College Park, MD, United States
⁶¹ Syracuse University, Syracuse, NY, United States
⁶² Pontifícia Universidade Católica do Rio de Janeiro (PUC-Rio), Rio de Janeiro, Brazil ^x
⁶³ University of Chinese Academy of Sciences, Beijing, China ^y
⁶⁴ Institute of Particle Physics, Central China Normal University, Wuhan, Hubei, China ^y
⁶⁵ Departamento de Física, Universidad Nacional de Colombia, Bogotá, Colombia ^z
⁶⁶ Institut für Physik, Universität Rostock, Rostock, Germany ^{aa}
⁶⁷ National Research Centre Kurchatov Institute, Moscow, Russia ^{ab}
⁶⁸ Instituto de Física Corpuscular (IFIC), Universitat de Valencia-CSIC, Valencia, Spain ^{ac}
⁶⁹ Van Swinderen Institute, University of Groningen, Groningen, The Netherlands ^{ad}

* Corresponding author.

E-mail address: lorenzo.capriotti@postgrad.manchester.ac.uk (L. Capriotti).

^a Universidade Federal do Triângulo Mineiro (UFMT), Uberaba-MG, Brazil.

^b Laboratoire Leprince-Ringuet, Palaiseau, France.

^c P.N. Lebedev Physical Institute, Russian Academy of Science (LPI RAS), Moscow, Russia.

^d Università di Bari, Bari, Italy.

^e Università di Bologna, Bologna, Italy.

^f Università di Cagliari, Cagliari, Italy.

^g Università di Ferrara, Ferrara, Italy.

^h Università di Genova, Genova, Italy.

ⁱ Università di Milano Bicocca, Milano, Italy.

^j Università di Roma Tor Vergata, Roma, Italy.

^k Università di Roma La Sapienza, Roma, Italy.

^l AGH – University of Science and Technology, Faculty of Computer Science, Electronics and Telecommunications, Kraków, Poland.

^m LIFAELS, La Salle, Universitat Ramon Llull, Barcelona, Spain.

ⁿ Hanoi University of Science, Hanoi, Viet Nam.

^o Università di Padova, Padova, Italy.

^p Università di Pisa, Pisa, Italy.

^q Università degli Studi di Milano, Milano, Italy.

^r Università di Urbino, Urbino, Italy.

^s Università della Basilicata, Potenza, Italy.

^t Scuola Normale Superiore, Pisa, Italy.

^u Università di Modena e Reggio Emilia, Modena, Italy.

^v Iligan Institute of Technology (IIT), Iligan, Philippines.

^w Novosibirsk State University, Novosibirsk, Russia.

^x Associated to Universidade Federal do Rio de Janeiro (UFRJ), Rio de Janeiro, Brazil.

^y Associated to Center for High Energy Physics, Tsinghua University, Beijing, China.

^z Associated to LPNHE, Université Pierre et Marie Curie, Université Paris Diderot, CNRS/IN2P3, Paris, France.

^{aa} Associated to Physikalisches Institut, Ruprecht-Karls-Universität Heidelberg, Heidelberg, Germany.

^{ab} Associated to Institute of Theoretical and Experimental Physics (ITEP), Moscow, Russia.

^{ac} Associated to ICCUB, Universitat de Barcelona, Barcelona, Spain.

^{ad} Associated to Nikhef National Institute for Subatomic Physics, Amsterdam, The Netherlands.

[†] Deceased.